AiMT Advances in Military Technology
Vol. 9, No. 1, June 2014

Prediction of the Air Gun Performance

V. Horák[1*], L. Do Duc[2], R. Vítek[3], S. Beer[3] and Q. H. Mai[4]

[1] *Department of Mechanical Engineering, University of Defence, Brno, Czech Republic*
[2] *Student of Faculty of Military Technology, University of Defence, Brno, Czech Republic*
[3] *Department of Weapons and Ammunition, University of Defence, Brno, Czech Republic*
[4] *Department of Weapons and Ammunition, Military Technical Academy, Hanoi, Vietnam*

The manuscript was received on 20 January 2014 and was accepted after revision for publication on 20 March 2014.

Abstract:

The article is focussed on the quasi-dynamic analysis of the air gun performance. The object of modelling is a comprehensive description of the thermodynamic processes taking place in different parts and working chambers of an air gun. Individual equations of the mathematical description are applications of the first law of thermodynamics, which is complemented by the state behaviour and the principles of air flow, including the critical flow. The boundary conditions of the solution of these equations are given by the design dimensions and weights of the gun moving components. The problem is solved using the MATLAB environment. The result of the solution represents the determination of the time courses of pressure in the different working chambers, including the power gas fluid forces acting on the gun moving components and the pellet. Results of the solution are compared with the measured pressure time dependence in the given working chamber and the pellet muzzle velocity of the paintball gun DYE, Proto Rail 2011.

Keywords:

Fluid dynamics, airsoft gun, paintball gun, gun performance

1. Introduction

Air guns use pressurized air or other gas to shoot the pellets, as well as to simulate realistic recoil and the slide cycling. These guns are designed to be non-lethal and are capable of automatic and semi-automatic operation. Compressed air powered guns are often used for airsoft, paintball, and target shooting sports or for hunting.

Paintball markers, also known as paintball guns, are used in the sport of paintball. Airsoft guns are replica firearms used in airsoft games, where combat situations are simulated. In the past, airsoft guns were used almost solely for recreational purposes,

[*] *Corresponding author: University of Defence, Kounicova 65, 662 10 Brno, Czech Republic, phone: +420 973 442 616, E-mail: vladimir.horak@unob.cz*

but in recent years the airsoft technology became adopted by many institutions as an extremely affordable and reliable tool for military and law enforcement training. Airsoft guns can be modified to increase the pellet velocity, the rate of fire, the number of shots, reliability, etc. The internal arrangement of components and ports of most air guns can be upgraded which can increase a gun performance significantly.

It would be advantageous to use a mathematical model of air gun having several chambers and considering interaction with the gun moving components and the pellet.

A simple physical analysis of a one-chamber air gun is provided in [1], where we can find reasonable approximations that permit a derivation of muzzle velocity. A gasdynamic-acoustic model of a simple air gun is given in [2]. The flow within the one-chamber gas gun is simulated using a quasi-one-dimensional Lagrangian compressible flow solver in [3] for subsonic and transonic flows.

The internal workings of a spring-air pellet gun is modelled in [4] for determining the ballistic performance and maximum internal gas pressure of a given gun design.

The more complex model of air gun is not available. Therefore, the objective of this study is to formulate the mathematical model which enables to predict the change of air gun performance due to change of gun design dimensions, weights of moving components, power gas pressure and temperature.

2. Principle of the Observed Air Gun Operation

Scheme of the given air gun is shown in Fig. 1. Air is supplied into two points on the breach, which is located at the rear of the barrel. The breach contains the can, the bolt and the manifold. At the back, the air is routed through the back cap and manifold and fills up the supply chamber around the manifold. In the front, the air is routed through the solenoid into the can. The bolt is kept in the back position by the air supplied into the can.

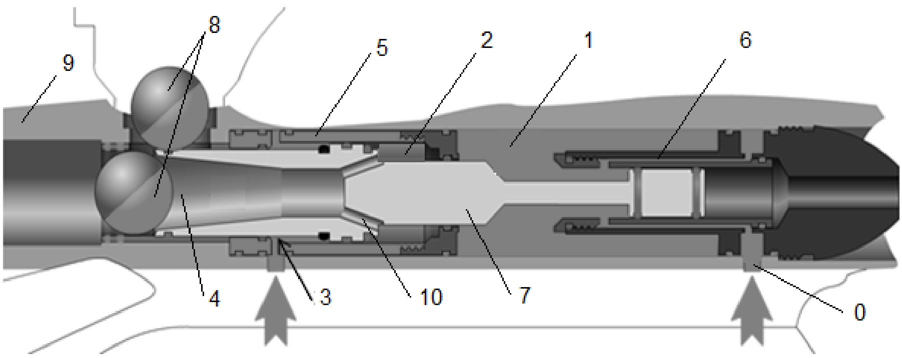

Fig. 1 Scheme of the air gun: 0 – back cap, 1 – supply chamber, 2, 3 – working chambers of the can, 4 – working chamber behind the pellet, 5 – can, 6 – manifold, 7 – bolt, 8 – pellet, 9 – barrel, 10 – valve of the bolt

If we suppose that the gun is loaded and aimed at the target, then the given air gun operation can be described in following way:

- The first phase of the gun operation begins when the trigger is pressed, the solenoid valve controlling the supply of compressed air is actuated and the air inside the can is discharged through the flow area A_{3a} from the working chamber 3 into surrounding atmosphere. The force created by the air inside the supply chamber 1 causes the bolt 7 to start moving forward. The first phase ends when the bolt 7 has slid about half way forward and the tail of the bolt has closed the air input 0 to the supply chamber 1 by closing the flow area A_{01} between the air input and the supply chamber.

- The second phase of the gun operation begins when the bolt continues in moving forward due to the expansion of the air within the supply chamber 1. This phase ends when the bolt 7 reaches the forward position and closes the barrel 9 of the gun. Now, the gun is ready to shoot.
- The third phase of the gun operation is when the bolt 7 has reached the forward point, the valve of the bolt 10 is opened and the air inside the supply chamber 1 discharges through the working chamber 2 of the can and through the flow area A_{24} into the working chamber 4 behind the pellet. Then the gas pressure force shoots the pellet 8 from the barrel 9.

After this the solenoid is deactivated and the air is supplied through the solenoid valve back into the working chamber 3. This causes the bolt 7 to return to the back position, therefore the flow area A_{01} between the air input 0 and the supply chamber 1 is opened and the supply chamber is to be re-charged. Thus, the gun is prepared for the next range and then the full cycle of gun can be repeated.

3. Mathematical Model of Simulation

The zero-dimensional model based on the mass and energy conservation [5] has been developed for the comprehensive simulation of the air gun operation. The exchange of mass and energy between the guns working chambers takes place in an open thermodynamic system (Fig. 2). Airflows indexed by *ij* enter and leave across the boundary of the system control volume.

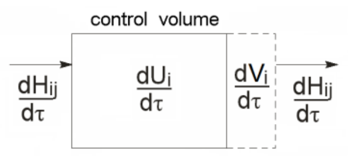

Fig. 2 Scheme of i-th thermodynamic system: $\mathrm{d}H_{ij}/\mathrm{d}\tau$ *– enthalpy rates crossing the boundary,* $\mathrm{d}U_i/\mathrm{d}\tau$ *– internal energy time change,* $\mathrm{d}V_i/\mathrm{d}\tau$ *– change of the system volume*

During the unsteady-state processes, when the state quantities of a system vary with time and also the state and the amount of incoming and outgoing air can vary with time, the first law of thermodynamics acquires the common differential rate form with respect to a time-lag $d\tau$ for the *i*-th working chamber

$$\sum_{ij} \frac{\mathrm{d}H_{ij}}{\mathrm{d}\tau} = \frac{\mathrm{d}U_i}{\mathrm{d}\tau} + \frac{\mathrm{d}W_i}{\mathrm{d}\tau}, \tag{1}$$

where a heat transfer between the control volume and its environment is neglected for the rapid processes of a gunshot.

The sum of enthalpy rates of airflows entering and leaving across the system boundary can be expressed by the air mass flow rates $\dot{m}_{ij}$ and the specific enthalpies h_{ij} as

$$\sum_{ij} \frac{\mathrm{d}\, H_{ij}}{\mathrm{d}\,\tau} = \sum_{ij} \dot{m}_{ij} h_{ij} \ . \tag{2}$$

The internal energy time change, which is given by the change of mass m_i and by the change of specific internal energy u_i inside the working chamber, thus

$$\frac{\mathrm{d}U_i}{\mathrm{d}\,\tau} = \frac{\mathrm{d}\left(m_i\, u_i\right)}{\mathrm{d}\,\tau} = \frac{\mathrm{d}\, m_i}{\mathrm{d}\,\tau} u_i + m_i \frac{\mathrm{d}\, u_i}{\mathrm{d}\,\tau} \ . \tag{3}$$

The volume boundary work is determined by the change of volume V_i as

$$\frac{\mathrm{d}W_i}{\mathrm{d}\,\tau} = p_i \frac{\mathrm{d}V_i}{\mathrm{d}\,\tau} \, , \tag{4}$$

where p_i is the pressure of air in the working chamber.

The change of a working chamber volume is given by the chamber cross-sectional area $A_{\mathrm{p}i}$ and the displacement x_i of system moving boundary (Fig. 2)

$$\frac{\mathrm{d}V_i}{\mathrm{d}\,\tau} = \frac{\mathrm{d}\left(A_{\mathrm{p}i} x_i\right)}{\mathrm{d}\,\tau} = A_{\mathrm{p}i} \frac{\mathrm{d}\, x_i}{\mathrm{d}\,\tau} = \upsilon_{\mathrm{p}i} A_{\mathrm{p}i} \, , \tag{5}$$

where $\upsilon_{\mathrm{p}i}$ is the velocity of the guns moving components such as the bolt or the pellet.

The change of the mass inside the each working chamber is given by the mass balance of the system control volume expressed in the rate form as summation of all the inlets and exits

$$\frac{\mathrm{d}\, m_i}{\mathrm{d}\,\tau} = \sum_{ij} \dot{m}_{ij} \ . \tag{6}$$

The mass airflow rate between the gun working chambers i and j is given by the air discharge through the nozzle of flow area A_{ij} as

$$\dot{m}_{ij} = C_{ij} \frac{\upsilon_{ij} A_{ij}}{v_{ij}} \, , \tag{7}$$

where υ_{ij} is the discharge airflow velocity, v_{ij} is the specific volume of air in the discharge opening, C_{ij} is the discharge coefficient; it is usually assumed that the discharge coefficient is between 0.45 – 0.61.

Saint-Venant and Wantzel's formula [6] for an ideal gas is used for determining the discharge airflow velocity under the specified value of pressure drop between working chambers i and j as

$$\upsilon_{ij} = \sqrt{\frac{2\kappa}{\kappa - 1} p_i\, v_i \left[1 - \left(\frac{p_j}{p_i} \right)^{\frac{\kappa-1}{\kappa}} \right]} \, , \tag{8}$$

where $\kappa = c_p / c_V \approx 1.4$ is the specific heat ratio.

Formula (8) is valid for subsonic flows. For supercritical pressure drops, the pressure of the air in the discharge opening p_j is equal to the critical pressure p_j*. That critical value can be calculated from the dimensionless critical pressure ratio equation [7], as follows

$$\frac{p_j{}^*}{p_i} = \left(\frac{2}{\kappa+1}\right)^{\frac{\kappa}{\kappa-1}} \approx 0.5283\,. \tag{9}$$

The specific volume v_{ij} of the air in the discharge port is given by the isentropic expansion

$$v_{ij} = v_i \left(\frac{p_i}{p_j}\right)^{\frac{1}{\kappa}}\,. \tag{10}$$

Regarding the usual values of power gas pressures and temperatures, the assumption of air as an ideal gas is fully acceptable. The relation between state quantities for the *i*-th working chamber is

$$p_i\,V_i = m_i\,r\,T_i\,, \tag{11}$$

where the air specific gas constant r = 287 J/(kg K). Further, assuming constant values of the specific heat capacities, the specific internal energy u_i and the specific enthalpy h_i can be simply expressed as

$$u_i = c_V\,T_i \qquad \text{and} \qquad h_i = c_p\,T_i\,. \tag{12}$$

3.1. Application of the First Law of Thermodynamics

By applying the First Law of Thermodynamics (1) for all air gun working chambers (see Fig. 1), we can obtain equations of the energy conservation for the supply chamber 1

$$\dot{m}_{01}h_0 - \dot{m}_{12}h_1 = \frac{\mathrm{d}\left(m_1 u_1\right)}{\mathrm{d}\,\tau} + p_1\,\frac{\mathrm{d}V_1}{\mathrm{d}\,\tau}\,, \tag{13}$$

for the working chambers 2 and 3 of the can

$$\dot{m}_{12}h_1 - \dot{m}_{24}h_2 = \frac{\mathrm{d}\left(m_2 u_2\right)}{\mathrm{d}\,\tau}\,, \tag{14}$$

$$-\dot{m}_{3\mathrm{a}}h_3 = \frac{\mathrm{d}\left(m_3 u_3\right)}{\mathrm{d}\,\tau} + p_3\,\frac{\mathrm{d}V_3}{\mathrm{d}\,\tau}\,, \tag{15}$$

and for the working chamber 4 behind the pellet

$$\dot{m}_{24}h_2 = \frac{\mathrm{d}\left(m_4 u_4\right)}{\mathrm{d}\,\tau} + p_4\,\frac{\mathrm{d}V_4}{\mathrm{d}\,\tau}\,. \tag{16}$$

Where individual mass airflow rates between given gun working chambers are determined by Eq. (7).
Note: According to the sign convention, the inlet mass flow rate is positive and the exit mass flow rate is negative.

3.2. Application of the Law of Mass Conservation

By applying the Law of Mass Conservation (6) for the given working chambers with an assumption that pressures $p_1 > p_2$, $p_2 > p_4$ and $p_3 > p_\mathrm{a}$, we can express the change in mass of the air within working chambers by using Eq. (7) as follows:

$$\frac{\mathrm{d}\,m_1}{\mathrm{d}\,\tau} = \dot{m}_{01} - \dot{m}_{12} = C_{01}\,\frac{\upsilon_{01}A_{01}}{v_{01}} - C_{12}\,\frac{\upsilon_{12}A_{12}}{v_{12}}\,, \tag{17}$$

$$\frac{\mathrm{d}\,m_2}{\mathrm{d}\,\tau} = \dot{m}_{12} - \dot{m}_{24} = C_{12}\,\frac{\upsilon_{12}A_{12}}{v_{12}} - C_{24}\,\frac{\upsilon_{24}A_{24}}{v_{24}}\,, \tag{18}$$

$$\frac{\mathrm{d}\,m_3}{\mathrm{d}\,\tau} = -\dot{m}_{3\mathrm{a}} = -C_{3\mathrm{a}}\,\frac{\upsilon_{3\mathrm{a}}A_{3\mathrm{a}}}{v_{3\mathrm{a}}}\,, \tag{19}$$

$$\frac{\mathrm{d}\,m_4}{\mathrm{d}\,\tau} = \dot{m}_{24} = C_{24}\,\frac{\upsilon_{24}A_{24}}{v_{24}}\,. \tag{20}$$

3.3. Solution of State Variables

By introducing Eqs. (3), (5), (12), and (17-20) into Eqs. (13-16) and by rearranging them, we obtain the change in temperature of the gas within the working chambers in the following forms

$$\frac{\mathrm{d}\,T_1}{\mathrm{d}\,\tau} = \frac{1}{m_1}\left[\dot{m}_{01}\kappa T_0 - \dot{m}_{12}\left(\kappa-1\right)T_1 - \dot{m}_{01}T_1 - \frac{p_1A_{\mathrm{p}1}\upsilon_{\mathrm{p}1}}{c_V}\right], \tag{21}$$

$$\frac{\mathrm{d}\,T_2}{\mathrm{d}\,\tau} = \frac{1}{m_2}\left[\dot{m}_{12}\kappa T_1 - \dot{m}_{24}\left(\kappa-1\right)T_2 - \dot{m}_{12}T_2\right], \tag{22}$$

$$\frac{\mathrm{d}\,T_3}{\mathrm{d}\,\tau} = \frac{1}{m_3}\left[-\dot{m}_{3\mathrm{a}}\left(\kappa-1\right)T_3 - \frac{p_3A_{\mathrm{p}3}\upsilon_{\mathrm{p}3}}{c_V}\right], \tag{23}$$

$$\frac{\mathrm{d}\,T_4}{\mathrm{d}\,\tau} = \frac{1}{m_4}\left[\dot{m}_{24}\kappa T_2 - \dot{m}_{24}T_4 - \frac{p_4A_{\mathrm{p}4}\upsilon_{\mathrm{p}4}}{c_V}\right], \tag{24}$$

where $A_{\mathrm{p}1}$ and $A_{\mathrm{p}3}$ are the cross-sectional areas of moving parts for appropriate working chambers, $A_{\mathrm{p}4}$ is the cross-sectional area of the pellet, $\upsilon_{\mathrm{p}1} = \upsilon_{\mathrm{p}3}$ is the velocity of the bolt, and $\upsilon_{\mathrm{p}4}$ is the velocity of the pellet. Appropriate pressures of air within the working chambers are solved by means of the ideal gas equation of state (11).

3.4. Application of the Newton's Second Law

We apply the Newton's Second Law of motion for the air gun moving components (see Fig. 1), i.e. the bolt and the pellet. Three forces are acting on the bolt during its moving forward (Fig. 3).

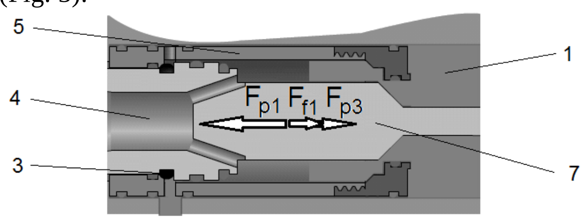

Fig. 3 Scheme of forces acting on the bolt

Two pressure forces F_{p1} and F_{p3} are acting on the bolt 7 in the supply chamber 1 and in the working chamber 3 against the atmospheric pressure, thus

$$F_{p1} = (p_1 - p_a)A_{p1} \quad \text{and} \quad F_{p3} = (p_3 - p_a)A_{p3}\,. \tag{25}$$

Third is the friction force F_{f1} acting in the O-ring sealing elements installed on the bolt and on the internal surfaces of the can 5 and the manifold 6, which is dependent upon the kinetic coefficient of friction and the ring material elasticity modulus [8]. The friction force in this case is supposed to be 10 % of sum of forces acting on the bolt 7.

Thus, we can apply the Newton's Second Law of motion for the bolt in the following form

$$a_{p1} = \frac{F_{p1} - F_{p3} - F_{f1}}{m_b + m_p} = 0.9\frac{F_{p1} - F_{p3}}{m_b + m_p}\,, \tag{26}$$

where a_b is the acceleration of the bolt, m_b is the mass of the bolt and m_p is the mass of the pellet.

For the linear motion, the bolt velocity v_{p1} is the rate of change of the bolt displacement x_{p1} and the bolt acceleration a_{p1} is the rate of change of the bolt velocity

$$v_{p1} = \frac{\mathrm{d}\,x_{p1}}{\mathrm{d}\,\tau} \quad \text{and} \quad a_{p1} = \frac{\mathrm{d}\,v_{p1}}{\mathrm{d}\,\tau}\,. \tag{27}$$

Two forces are acting on the pellet during its moving in the barrel (Fig. 4).

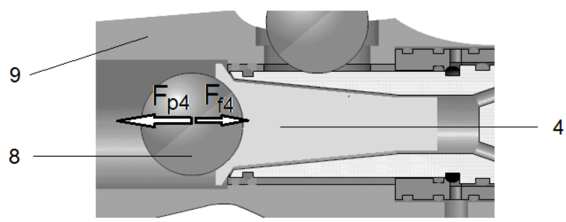

Fig. 4 Scheme of forces acting on the pellet

The pressure force F_{p4} acting on the pellet 8 due to air pressure in the working chamber 4 behind the pellet against the atmospheric pressure is

$$F_{p4} = (p_4 - p_a)A_{p4}\,. \tag{28}$$

And the friction force F_{f4} can be neglected for the smooth bore. Then the acceleration of the pellet a_{p4} is given by the acting of the pressure force F_{p4} on the pellet of mass m_p as

$$a_{p4} = \frac{\mathrm{d}\,v_{p4}}{\mathrm{d}\,\tau} = \frac{(p_4 - p_a)A_{p4}}{m_p} \quad \text{and} \quad v_{p4} = \frac{\mathrm{d}\,x_{p4}}{\mathrm{d}\,\tau}\,, \tag{29}$$

where v_{p4} is the pellet velocity and x_{p4} is the pellet displacement.

4. Results of Solution

The mathematical model described above has been solved by numerical integration using the MATLAB code by the explicit fourth-order Runge-Kutta method. Boundary conditions of differential equations are fully defined for the above described phases of the air gun operation. The solution ends at the time when the pellet leaves the barrel. In this moment, the muzzle velocity of the pellet is reached.

Results of the air gun performance represent the time courses of pressure and temperature in all working chambers during the gun cycle. Further, the power gas fluid forces acting on the gun bolt and the pellet are solved. Thus, the time courses of the bolt and the pellet velocity and the displacement can be calculated. The resulting value of pellet muzzle velocity is one of main parameters in evaluating the gun performance.

The input data of the solution for the paintball gun Proto Rail 2011 are given in Tab. 1. These input data include:

- Design parameters of the gun: areas between working chambers and appropriate discharge coefficients, the barrel length, the mass of the bolt and the pellet.
- Initial operating conditions of the solution: values of pressure and temperature in working chambers.

Tab. 1 Input data for the paintball gun Proto Rail 2011

Parameter	Value	Parameter	Value
A_{01}	2.50×10^{-5} m^2	C_{24}	0.5
A_{12}	1.13×10^{-4} m^2	C_{3a}	0.5
A_{24}	5.10×10^{-5} m^2	m_b	2.6×10^{-2} kg
A_{3a}	5.02×10^{-5} m^2	m_p	3.2×10^{-3} kg
A_{p1}	1.05×10^{-4} m^2	p_0	2.5 MPa
A_{p3}	1.19×10^{-4} m^2	p_{01}	1.07 MPa
A_{p4}	1.81×10^{-3} m^2	T_a	288 K
C_{01}	0.5	p_a	0.1 MPa
C_{12}	0.5	L	0.3 m

Results of the solution for the given example are clearly shown in Fig. 5 and Fig. 6, where we can see time courses of pressure and temperature in all gun working chambers.

The algorithm of the solution includes conditions for particular phases of the gun operation. These three phases are also seen in Fig. 5 and Fig. 6.

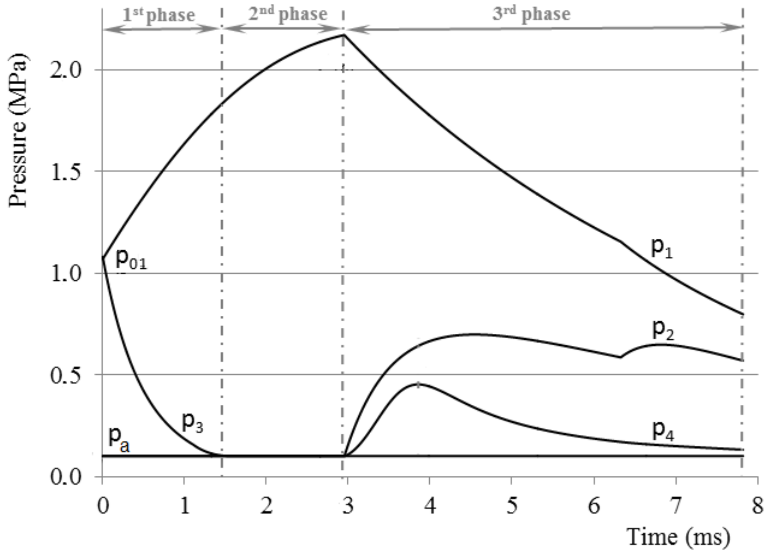

Fig. 5 Time courses of pressure in the gun working chambers for the paintball gun Proto Rail 2011

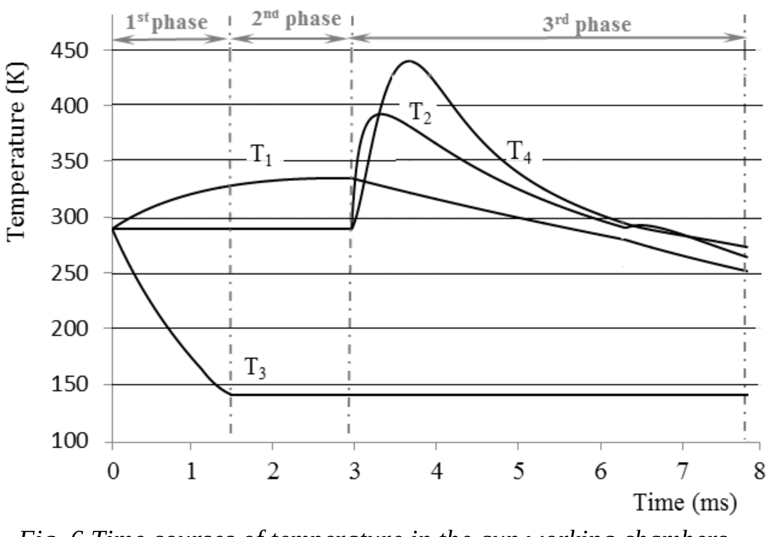

Fig. 6 Time courses of temperature in the gun working chambers for the paintball gun Proto Rail 2011

Courses of the pressure behind the pellet and the pellet velocity are the most significant parameters of the air gun performance. These courses of pressure behind the pellet and the pellet velocity related to the pellet displacement are shown in Fig. 7.

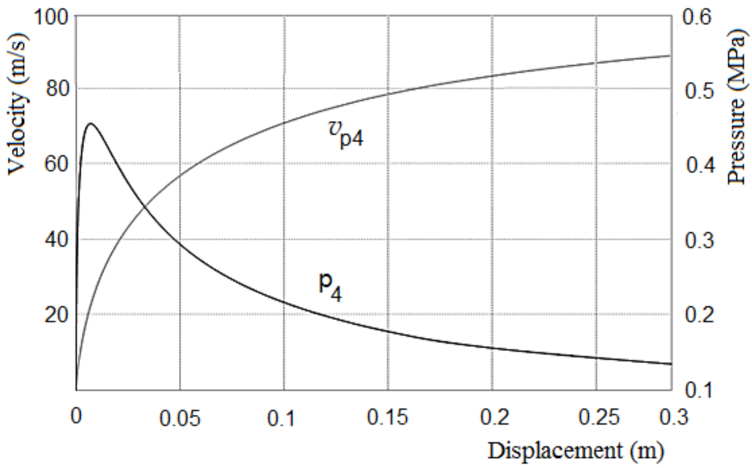

Fig. 7 Pressure behind the pellet and the pellet velocity related to the pellet displacement for the paintball gun Proto Rail 2011

The algorithm of the solution provides the muzzle velocity when the pellet leaves the barrel muzzle. The barrel length of the given paintball gun $L = 0.3$ m. For the given application (Fig. 7), the muzzle velocity $v = 88$ m/s.

5. Verification of the Mathematical Model

Results of the solution of pressure behind the pellet and the muzzle velocity are compared with the measured values. The comparison of calculated and measured time courses of pressure behind the pellet is shown in Fig. 8.

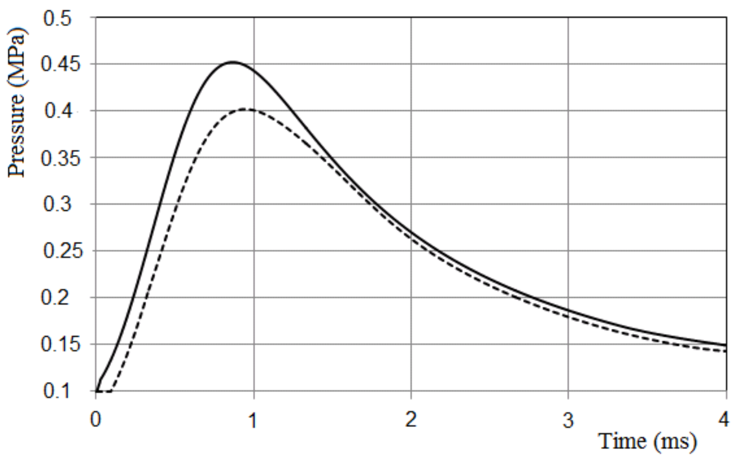

Fig. 8 Comparison of calculated (solids line) and measured (dashed line) time courses of pressure behind the pellet for the paintball gun Proto Rail 2011

Measurement of the time dependence of pressure behind the pellet has been performed in the experimental ballistic laboratory of the Department of Weapons and

Ammunition using the Kistler quartz high-pressure sensor model 6215. This sensor was attached to the working chamber behind the pellet by a special adapter. The mounting location of the pressure sensor on the gun is shown in Fig. 9.

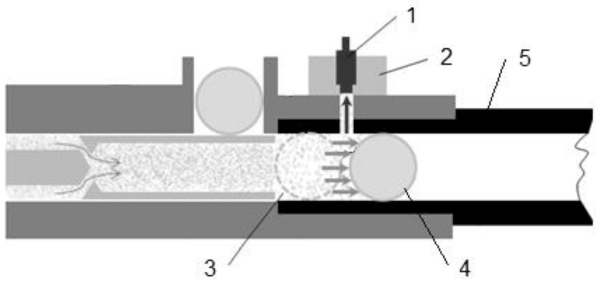

Fig. 9 Mounting location of the pressure sensor: 1 – high-pressure sensor, 2 – adapter, 3 – pellet initial position, 4 – pellet 5 – barrel

The sampling frequency of the analog-digital converter, which was used for the pressure course record, was set to 500 kHz.

The output signal has been filtered and smoothed (see Fig. 8) using the low-pass digital Butterworth filter of the 3rd order with the cut-off frequency f_n = 750 Hz in MATLAB.

The pellet velocity was measured in the experimental ballistic tunnel by using two pairs of optical light gates LS-04 (Prototypa-ZM, s.r.o), which were located at the distances of 2 m and 4.5 m from the gun's muzzle. The velocity of the pellet drops off steadily because of air resistance. Therefore, the initial velocity [9] is extrapolated by examining the values of both optical gates (see Tab. 2). The concept of ballistic coefficient [10] was applied for this extrapolation.

Tab. 2 Comparison of calculated and measured values of muzzle velocity

Measured pellet velocity – gate 1	Measured pellet velocity – gate 2	Extrapolated initial velocity	Calculated muzzle velocity
79.9 m/s	74.0 m/s	84.9 m/s	88 m/s

It can be stated that the results of solution are in a good agreement to the measured values.

The difference between calculated and measured time courses of pressure behind the pellet is given by the delay due to the pressure sensor location close to the pellets initial position.

Further, the slight disproportion between the calculated muzzle velocity and extrapolated initial velocity is probably given by neglecting the friction force and the air leakage between the pellet and barrel during the shot.

6. Prediction of the Air Gun Performance

Gun performance (such as the muzzle velocity, the kinetic energy, the shot-to-shot time, etc.) can be predicted either by the direct calculation from the model, or by using the influence coefficients which represent the partial response of the model due to the unit change in particular input parameters. Influence coefficients enable us to predict the change in any gun performance quantity $\delta f_i(x)$ due to the change in input parameters δx_{ik} (design parameters and initial conditions) by using the sum of partial changes [9]. Thus, the general equation for influence coefficients is

$$\frac{\delta f_i(x)}{f_i(x)} = \sum_k \Delta f_{ik} \frac{\delta x_k}{x_k}, \tag{30}$$

where subscript i denotes the output parameter and subscript k denotes the variable input quantity.

In the case of using the influence coefficients for the change in muzzle velocity v, the general equation (30) could be rewritten as

$$\frac{\delta v}{v} = \sum_k \Delta v_k \frac{\delta x_k}{x_k}. \tag{31}$$

The example of influence coefficients for the change in muzzle velocity for the observed paintball gun is given in Tab. 3. These values provide us with a clear view on mutual relations between individual parameters.

Tab. 3 Influence coefficients for the paintball gun Proto Rail 2011

Input parameters	Unit change	Change in muzzle velocity Δv_k [%]
Δp_0	+1 %	+0.0325
Δp_{01}	+1 %	+0.4339
Δm_{b}	+1 %	+0.0651
Δm_{p}	+1 %	–0.2495
ΔA_{24}	+1 %	+0.4300
ΔL	+1 %	+0.1410
ΔT_{a}	+1 %	+0.3146
Δp_{a}	+1 %	–0.3038

Thus, the change in the muzzle velocity δv for input parameters outlined in Tab. 3 can be expressed by

$$\begin{aligned}\frac{\delta v}{v} = {} & \Delta v_{p_0} \frac{\delta p_0}{p_0} + \Delta v_{p_{01}} \frac{\delta p_{01}}{p_{01}} + \Delta v_{m_{\mathrm{b}}} \frac{\delta m_{\mathrm{b}}}{m_{\mathrm{b}}} + \Delta v_{m_{\mathrm{p}}} \frac{\delta m_{\mathrm{p}}}{m_{\mathrm{p}}} + \\ & + \Delta v_{A_{24}} \frac{\delta A_{24}}{A_{24}} + \Delta v_L \frac{\delta L}{L} + \Delta v_{T_{\mathrm{a}}} \frac{\delta T_{\mathrm{a}}}{T_{\mathrm{a}}} + \Delta v_{p_{\mathrm{a}}} \frac{\delta p_{\mathrm{a}}}{p_{\mathrm{a}}}.\end{aligned} \tag{32}$$

As an example of using the influence coefficients, let us determine the change of the initial pressure δp_{01} in the supply chamber due to the change in atmospheric temperature by δT_a = 40 °C, provided that the muzzle velocity should remain unchanged ($\delta v = 0$), then yields

$$0 = \Delta v_{p_{01}} \frac{\delta p_{01}}{p_{01}} + \Delta v_{T_\mathrm{a}} \frac{\delta T_\mathrm{a}}{T_\mathrm{a}}$$
$$\Rightarrow \delta p_{01} = -\frac{\Delta v_{T_\mathrm{a}}}{\Delta v_{p_{01}}} \frac{\delta T_\mathrm{a}}{T_\mathrm{a}} p_{01} = -\frac{0.3146}{0.4339}\frac{40}{288} 1.07 = -0.108\,\mathrm{MPa} \tag{33}$$

The input data of design parameters and operating conditions for the paintball gun Proto Rail 2011 are given in Tab. 1.

7. Conclusions

In this study, the mathematical model of the air gun operation has been developed. The problem was solved using the MATLAB and the user program was compiled. It has been demonstrated that the results of the solution correspond very well with the experimental data of the course of pressure behind the pellet and the muzzle velocity.

Therefore, the presented simulation algorithm can become a powerful tool for analysing the processes of internal ballistics in a wider range of applications. The analysis enables us to understand how various design parameters and operating conditions influence the performance of air guns.

The gun's simulation algorithm may be applied in predicting and improving the air guns performance. Optionally, it may be used for optimization purposes.

The developed computer program could serve very well in an industrial design environment for the sector of the air arms' industry.

References

[1] DENNY, M. The Internal Ballistics of an Air Gun. *The Physics Teacher*. Vol. 49, February 2011, p. 81-83. ISSN 0031-921X.

[2] RIENSTRA, SW. *A Gasdynamic-Acoustic Model of a Bird Scare Gun. Mathematical Modeling: Case Studies from Industry*. New York: Cambridge University Press, 2000, p. 253-269.

[3] JOHNSTON, I. A. and KRISHNAMOORTHY, L. V. *A Numerical Simulation of Gas Gun Performance*. [Report DSTO-TN-0804]. Edinburgh: Defence Science and Technology Organisation, February 2008, 18 p.

[4] COMPTON, S. J. *Internal Ballistics of a Spring-Air Pellet Gun*. Available from <http://home2.fvcc.edu/~dhicketh/DiffEqns/spring07projects/StephenCompton/SpringAirModel.pdf>, 05/18/2007, 22 p.

[5] HORÁK, V. and KULISH, VV. *Thermodynamics*. Brno: University of Defence, 2011, 102 p. ISBN 978-80-7231-793-6.

[6] ARSENJEV, SL., LOZOVITSKI IB. and SIRIK, YP. *The Flowing System Gasdynamics*. Part 3: Saint-Venant – Wantzel's formula modern form. Available from <http://arxiv.org/ftp/physics/papers/0302/0302038.pdf>, February 2003, 3 p.

[7] POTTER, MC. and WIGGERT, DC. *Mechanics of Fluids*, 2nd edition. New Jersey: Prentice Hall, 1997, 689 p. ISBN 0-13-207622-5.

[8] AL-GHATHIAN, FM. and TARAWNEH, MS. Friction Forces in O-ring Sealing. *American Journal of Applied Sciences*, 2005, vol. 2, no. 3, p. 626-632. ISSN 1546-9239.

[9] PLÍHAL, B., BEER, S., KOMENDA, J., JEDLIČKA, L. and KUDA, B. *Ballistics* [In Czech]. Brno: Vojenská akademie v Brně, 2003.

[10] WRIGHT, M. The Ballistic Coefficient Explained. *Airgun World*, 2003, vol. 26, no. 1, p. 73-75. ISSN 0143-8255.

Acknowledgement

The work presented in this article has been supported by the institutional funding PRO K216 "Support of Research, Experimental Development, and Innovation in Mechanical Engineering" and by the Specific Research Support Project of the Faculty of Military Technology SV K201.